

Supplementary material for the paper ‘Nonlinear Plasmonic Cloaks to Realize Giant All-Optical Scattering Switching’

a) Influence of losses

After introducing realistic silver losses in the subwavelength plasmonic shell of Fig. 1(a), $\gamma = 4.35$ THz [16], we choose a slightly larger particle with $a = 45$ nm and $\eta_c = 0.2$. Moreover, we consider a higher, but still realistic nonlinear susceptibility values with $\chi^{(3)} = 4.4 \times 10^{-18} \text{ m}^2 / \text{V}^2$ [17]. In Fig. S1 we plot the calculated normalized SCS for input pump intensity $I_{in} = 1700 \text{ MW} / \text{cm}^2$. The Fano-type resonance is broader than in the lossless limit, as expected, and the field in the core is obviously less intense. However, even after considering realistic losses, bistable scattering response is achieved with a moderate all-optical switching and Fano-like SCS signature at the design frequency. The calculated unstable branch is plotted with a dotted line. We show in the insets the corresponding field distributions in the two scattering states.

To understand the transition between lossless and lossy limits, we use the same dimensions and nonlinear material at the core but we consider reduced losses $\gamma = 2.175$ THz in Fig. S2. The bistable scattering performance is plotted for a relatively low input pump intensity $I_{in} = 658 \text{ MW} / \text{cm}^2$. Again, bistable scattering response is achieved with a larger all-optical switching response at the design frequency, compared to the realistic silver loss case. This shows that the proposed structure can behave as an efficient all-optical switch and nanomemory, even when realistic losses are considered.

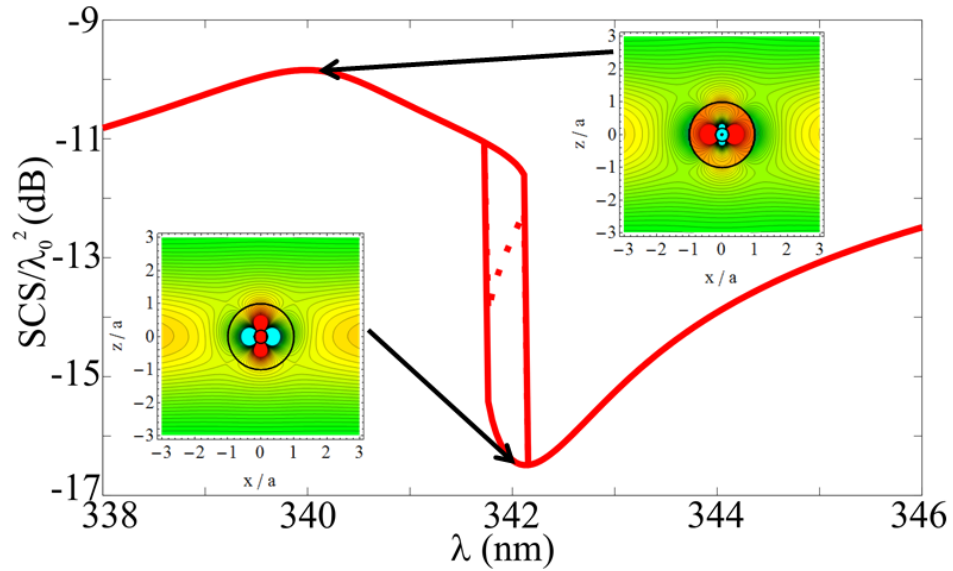


Figure S1 – Normalized SCS versus wavelength for a lossy plasmonic nonlinear cloak with an input intensity $I_{in} = 1700 \text{ MW} / \text{cm}^2$ and $\gamma = 4.35 \text{ THz}$. The distribution of the electric field (snapshot in time) for resonant scattering (left inset) and cloaking (right inset) wavelengths are also shown. The impinging plane wave travels from bottom to top.

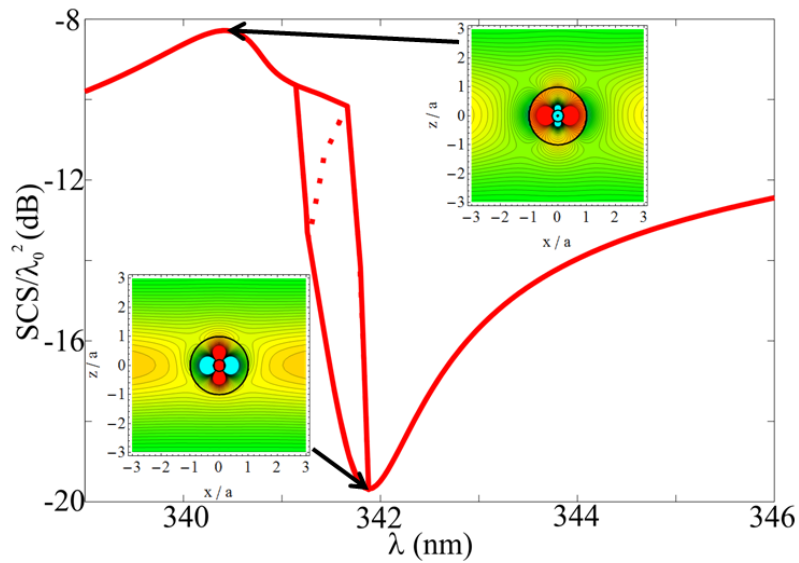


Figure S2 – Similar to Fig. S1, normalized SCS versus wavelength for a lossy plasmonic nonlinear cloak with an input intensity $I_{\text{in}} = 658 \text{ MW / cm}^2$ and $\gamma = 2.175 \text{ THz}$.

b) Field enhancement in the core and corresponding nonlinear permittivity variation

In Fig. S3, we show the mean value of the magnitude of the complex electric field, normalized to the impinging one in the core for the nanoparticle of Fig. 1 (blue line), compared with the mean value of the magnitude of the complex scattered electric field just outside the nanoparticle (red line) in the frequency range in which the Fano-type response is achieved [see Fig. 1(c)]. Point I in Fig. S3 corresponds to the resonant bright state, similar to Figs. 1-2. In a similar manner, point II in Fig. S3 corresponds to the cloaking state. Remarkably, the scattered fields experience a strong, Fano-type dispersion, as discussed in the paper, whereas the fields in the core are more uniformly enhanced, even in the cloaking state (point II). This clearly demonstrates that the weak nonlinear effects in the core may be strongly enhanced across the whole range of Fano-like response due to plasmonic effects, in order to realize giant all-optical switching in a single nanoparticle.

The variation of the core's nonlinear permittivity with impinging light intensity for the nonlinear lossless plasmonic cloak considered in the manuscript is shown in Fig. S4. The permittivity shows strong bistable dispersion, as expected. Small permittivity variations are required to trigger the nonlinear response, corresponding to moderate input pumping intensities.

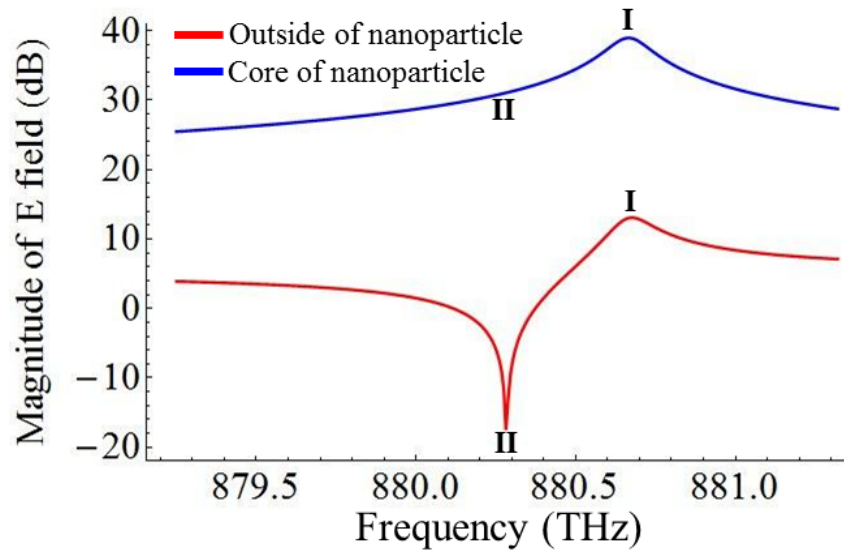


Figure S3 – Average magnitude of the electric field, normalized to the impinging one, inside the core (blue line) and the scattered component just outside the shell (red line).

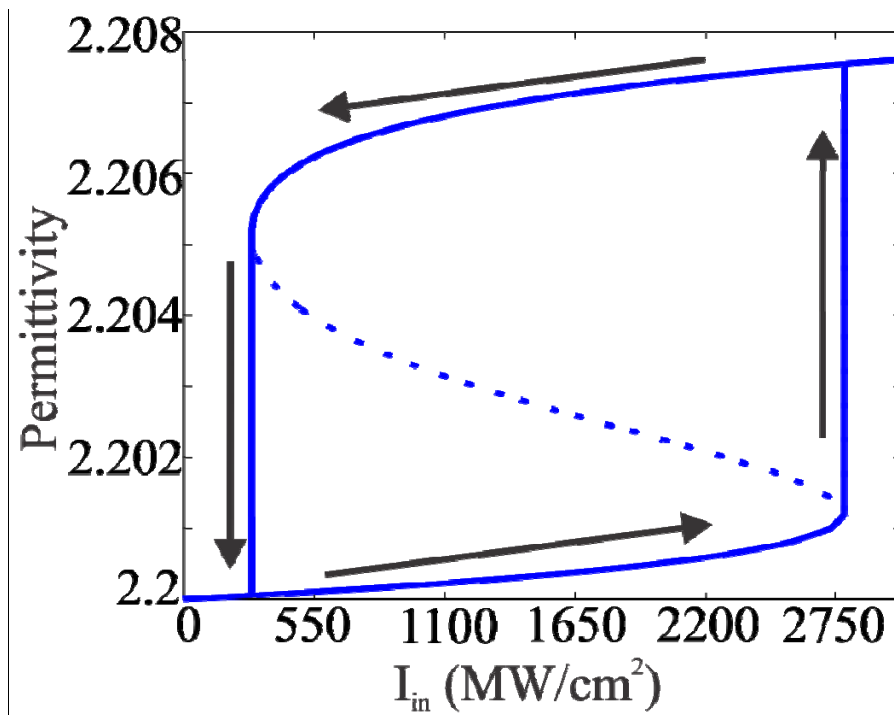


Figure S4 – Variation of relative nonlinear permittivity of the core with the impinging intensity.

The unstable branch is shown with a dotted line.

c) Collection of nonlinear nanoparticles

A planar array of nonlinear nanoparticles is considered here, as shown in Fig. S5. Each nanoparticle has parameters and dimensions similar to Fig. 3. The array has square lattice with periodicity $d_x = d_y = 2.25a$, where a is the radius of each nanoparticle. The reflection and transmission coefficients from this metasurface are shown in Fig. S6, both for linear (blue line) and nonlinear (red line) operations. The metasurface has a sharp signature similar to each individual nanoparticle. When nonlinearities are introduced, giant switching operation is realized with a moderate pumping intensity $I_m = 200 \text{ MW} / \text{cm}^2$. Integrated planarized optical nanodevices may be realized with the proposed metasurface, working as efficient all-optical switches and memories.

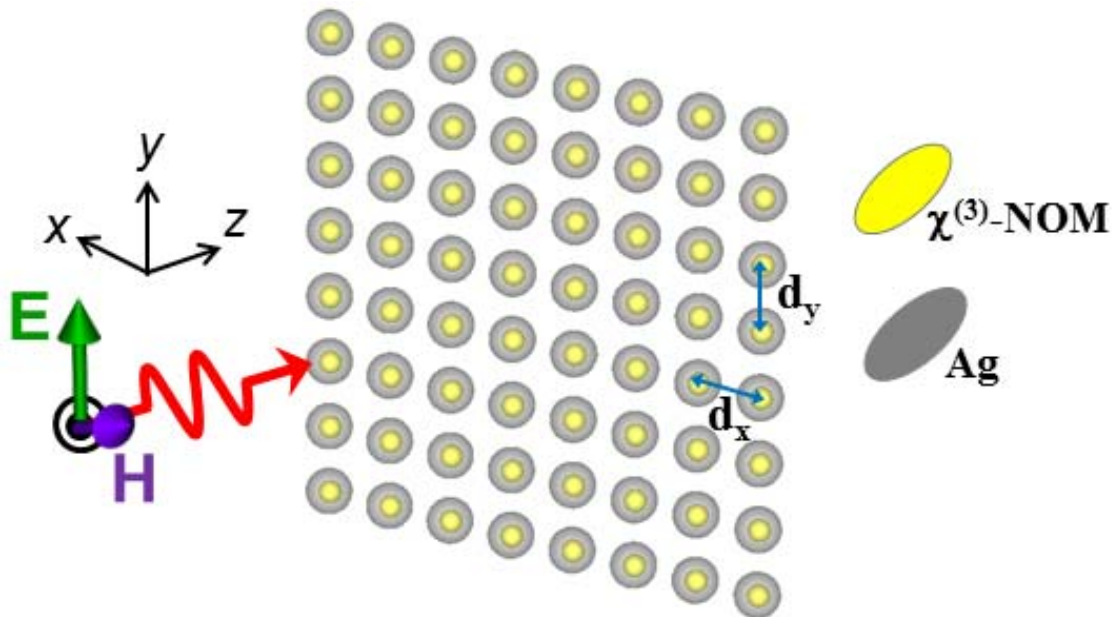


Figure S5 – A periodic array of nanoswitches. Each nanoparticle has similar parameters and dimensions as the one presented in Fig. 3.

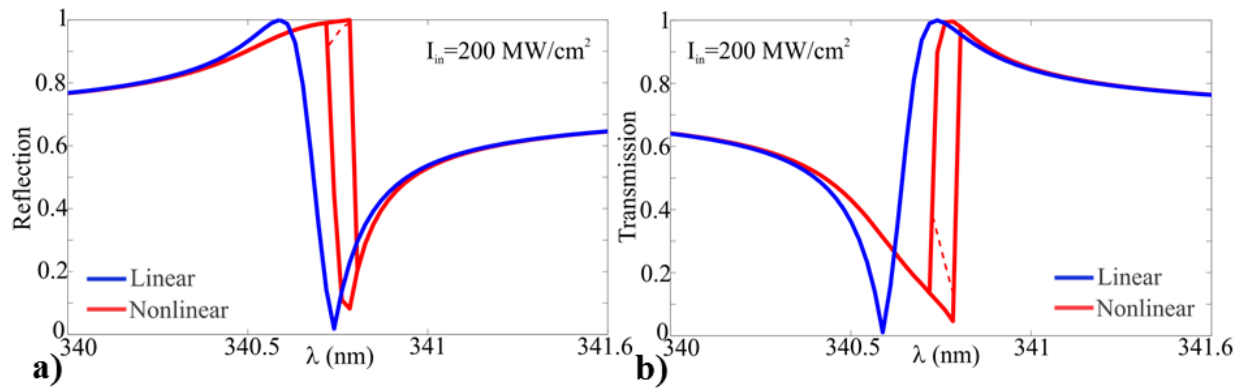


Figure S6 – a) Reflection and b) transmission of the metasurface shown in Fig. S5 for linear (blue line) and nonlinear (red line) operations. The unstable branches of the bistable curves are shown with the dashed red lines.